

BEAM: Binary Expert Activation Masking for Dynamic Routing in MoE

Juntong Wu^{1,2,*}, Jialiang Cheng^{1,*}, Qishen Yin², Yue Dai¹,
Yuliang Yan¹, Fuyu Lv¹, Ou Dan¹, Li Yuan²

¹ Taobao & Tmall Group of Alibaba

² Shenzhen Graduate School, Peking University

Correspondence: jichen.cjl@alibaba-inc.com, yuanli-ece@pku.edu.cn

Abstract

Mixture-of-Experts (MoE) architectures enhance the efficiency of large language models by activating only a subset of experts per token. However, standard MoE employs a fixed Top-K routing strategy, leading to redundant computation and suboptimal inference latency. Existing acceleration methods either require costly retraining with architectural changes or suffer from severe performance drop at high sparsity due to train-inference mismatch. To address these limitations, we propose **BEAM** (Binary Expert Activation Masking), a novel method that learns token-adaptive expert selection via trainable binary masks. With a straight-through estimator and an auxiliary regularization loss, BEAM induces dynamic expert sparsity through end-to-end training while maintaining model capability. We further implement an efficient custom CUDA kernel for BEAM, ensuring seamless integration with the vLLM inference framework. Experiments show that BEAM retains over 98% of the original model’s performance while reducing MoE layer FLOPs by up to 85%, achieving up to $2.5\times$ faster decoding and $1.4\times$ higher throughput, demonstrating its effectiveness as a practical, plug-and-play solution for efficient MoE inference. Code implementation of BEAM can be found in <https://github.com/Time-Rune/BEAM>.

1 Introduction

Mixture-of-Experts (MoE) enables efficient scaling through sparse activation, where each token is processed by only a small subset of specialized feed-forward network (FFN) experts [Yang et al., 2025a, Liu et al., 2024a, Jiang et al., 2024]. The dominant paradigm for expert selection is the fixed Top-K routing mechanism, which selects the K experts with the highest router logits for each token [Shazeer et al., 2017, Lepikhin et al., 2020]. While simple and widely adopted, it ignores token-level complexity, leading to redundant computation for simple tokens [Huang et al., 2024, Zeng et al., 2024]. This inefficiency ultimately limits the potential for faster MoE model inference.

To address the inefficiency of fixed Top-K routing, recent work has explored dynamic expert activation, falling into three categories.

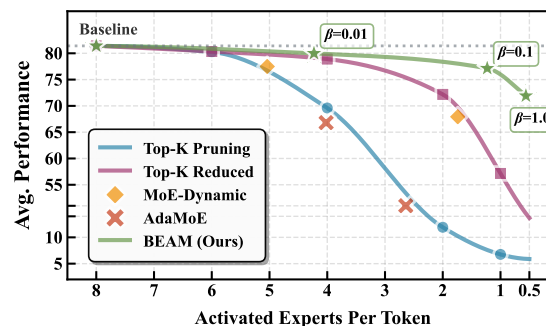


Figure 1: Performance-sparsity trade-off of BEAM and baselines on Qwen3-30B-A3B.

* Equal contribution ✉ Corresponding author

The first modifies the routing logits to enable token-adaptive expert counts [Huang et al., 2024, Lu et al., 2024, Yang et al., 2024b, Aghdam et al., 2024, Guo et al., 2024], but fails to skip redundant high-weight experts and enforces a minimum activation floor, limiting achievable sparsity. The second introduces special experts such as zero-computation null experts to control sparsity [Zeng et al., 2024, Jin et al., 2024, Gui et al., 2025], yet requires additional hyperparameters and complicated fine-tuning process, and only enables passive, indirect sparsity control. The third merges or prunes experts statically [Chen et al., 2025, Liu et al., 2024b, Yang et al., 2024a], but cannot adapt to input complexity at inference time and often suffers from severe performance degradation at high sparsity levels.

In this work, we propose **BEAM (Binary Expert Activation Masking)**, a novel dynamic routing framework designed to achieve extreme expert sparsity and inference speedups in MoE models. As shown in Figure 2, BEAM introduces a lightweight, learnable mask router that generates a binary mask applied to the top-K candidate experts from the primary router, selectively deactivating redundant ones. Sparsity is encouraged via an auxiliary regularization loss, and gradients are propagated through the binary mask using the straight-through estimator (STE) [Bengio et al., 2013]. Crucially, BEAM decouples sparsity control from expert selection. The primary router still handles load balancing and expert choice, while the mask router solely determines activation count. This separation avoids conflicts and enables more activation patterns within the Top-K candidate set, providing fine-grained, token-adaptive sparsity control that fixed Top-K or logits-based methods cannot express. To demonstrate the practical impact, we integrate BEAM into vLLM [Kwon et al., 2023] through a custom CUDA kernel, requiring only a single-line change and delivering significant real-world speedups, which makes BEAM a practical, plug-and-play solution for efficient MoE deployment.

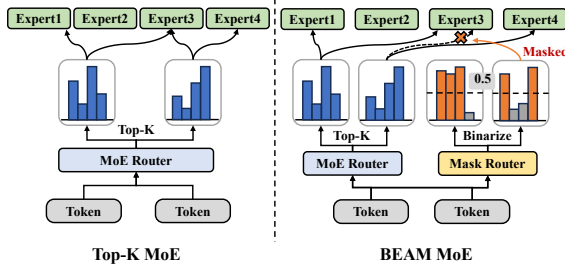


Figure 2: Vanilla Top- K vs. BEAM: BEAM learns a binary mask over Top- K candidates for token-adaptive activation.

Our contributions are summarized as follows:

- We propose BEAM, a novel dynamic routing framework that achieves extreme expert sparsity via a learnable mask router. It directly prunes redundant experts from the Top-K set for token-adaptive computation, in contrast to existing indirect or post-hoc approaches.
- We provide a practical, plug-and-play deployment solution by integrating BEAM into vLLM through a custom CUDA kernel, requiring minimal code changes.
- Extensive experiments show BEAM preserves over 98% of performance while reducing MoE layer FLOPs by up to 85% (Figure 1), yielding $1.4\times$ higher throughput and $2.5\times$ faster decoding.

2 Related Work

Routing Logits Modification These methods modify routing logits to enable token-adaptive expert counts. MoE-Dynamic [Huang et al., 2024] and XMoE [Yang et al., 2024b] activate experts until the cumulative probability exceeds a threshold. DTop-p [Jin et al., 2025] improves MoE-Dynamic by replacing the fixed threshold with a learnable sparsity controller. Adaptive Gating [Li et al., 2023b] and NAAE [Lu et al., 2024] dynamically switches between Top-1 and Top-2 based on the gap between the top two logits. DA-MoE [Aghdam et al., 2024] computes token importance from attention scores to allocate a dynamic Top-K. DynMoE [Guo et al., 2024] replaces the softmax router with per-expert sigmoid gates. MaskMoE [Su et al., 2024] employs static vocabulary-based masks derived from pretraining data distributions to improve rare-token expert assignment. However, most of them rely on the unverified heuristic that low entropy of routing logits implies fewer needed experts, fail to skip redundant high-weight experts, and require at least one active expert, preventing acceleration.

Special Experts These methods reduce FLOPs by routing tokens to experts that incur no computation. AdaMoE [Zeng et al., 2024] introduces null experts that outputs zero. LongCat [Gui et al., 2025] uses zero-computation experts that return the input as their output. MoE++ [Jin et al., 2024] extended this idea with three types of zero-computation experts. However, these methods introduce extra

hyperparameters and achieve sparsity indirectly via passive placeholder routing rather than explicit expert minimization, undermining plug-and-play usability.

Static Expert Merging and Pruning These training-free methods reduce redundancy by merging or pruning experts. DEK [Zhang et al., 2025] groups similar experts in feature space and merges experts in each group. EEP [Liu et al., 2024b] utilizes a gradient-free evolutionary search to determine pruning and merging patterns. MC-SMoE [Li et al., 2023c] leverages routing statistics to guide expert merging and decomposes the merged experts into low-rank and structural sparse alternatives. HC-SMoE [Chen et al., 2025] applies hierarchical clustering on expert outputs to merge experts. However, these methods cannot adapt to the varying complexity of input tokens at inference time and often suffer performance degradation under high compression.

3 Method

3.1 Preliminaries and Motivation

MoE replaces dense FFN layers with N expert networks $\{\mathcal{E}_1, \dots, \mathcal{E}_N\}$ and a router \mathcal{R} . Given an input token $\mathbf{x} \in \mathbb{R}^{d_h}$, the router computes logits $\mathbf{r} = \mathcal{R}(\mathbf{x}) \in \mathbb{R}^N$, which are converted into routing weights via softmax. Under standard Top-K routing, only the K experts with the largest routing logits are activated. Specifically, the $\text{Top-}K(\cdot)$ operator retains the K largest values in \mathbf{r} and sets the remaining entries to $-\infty$, yielding routing weights:

$$\mathbf{g}_i = \text{Softmax}(\text{Top-}K(\mathbf{r}))_i. \quad (1)$$

The MoE output is a weighted sum of expert outputs:

$$\mathbf{y} = \sum_{i=1}^N \mathbf{g}_i \cdot \mathcal{E}_i(\mathbf{x}), \quad (2)$$

where each expert \mathcal{E}_i typically follows a Gated Linear Unit (GLU) structure:

$$\mathcal{E}_i(\mathbf{x}) = \left(\delta(\mathbf{x}\mathbf{W}_{\text{gate}}^{(i)}) \odot (\mathbf{x}\mathbf{W}_{\text{up}}^{(i)}) \right) \mathbf{W}_{\text{down}}^{(i)}. \quad (3)$$

Although Top-K routing enables scalable training, it assigns a uniform computational budget to all tokens, causing redundancy for simple ones.

Existing dynamic routing methods attempt to address this problem but remain limited in practice. First, these approaches implicitly treat routing rank as a proxy for expert importance. However, a lower-ranked expert can still be critical for a given token while a high-weight one may be redundant, which is empirically validated in Section 5.2 and Appendix B.4. Second, cumulative probability thresholds and null experts cannot actively prune redundant experts, limiting compression ratios (Section 4.2). Third, these methods entangle expert selection, load balancing, and sparsity control in a single router, creating inherent gradient conflicts, thereby degrading model capacity (Section 4.2).

3.2 BEAM: Binary Expert Activation Masking

The above limitations motivate BEAM, which enables token-adaptive expert activation by introducing a lightweight and learnable mask router that generates a binary mask to selectively deactivate redundant experts from the standard Top-K candidate set, as shown in Figure 3. Formally, given an input token embedding $\mathbf{x} \in \mathbb{R}^{d_h}$, BEAM operates in four steps.

Step 1: Standard Top-K Routing. The primary router \mathcal{R} computes logits $\mathbf{r} = \mathcal{R}(\mathbf{x}) \in \mathbb{R}^N$, where N is the total number of experts. The $\text{Top-}K(\cdot)$ operator retains the K largest values and sets the rest to $-\infty$. The normalized routing weights are computed as:

$$\mathbf{g}_i = \text{Softmax}(\text{Top-}K(\mathbf{r}))_i, \quad i = 1, \dots, N, \quad (4)$$

where $\mathbf{g}_i > 0$ only for the top K experts and $\sum_{i=1}^N \mathbf{g}_i = 1$.

Step 2: Raw Mask Generation. A lightweight auxiliary mask router, parameterized by $\mathbf{W}_m \in \mathbb{R}^{d_h \times N}$, processes the same input token \mathbf{x} to generate a raw mask $\hat{\mathbf{m}}$. We apply a Sigmoid activation σ to constrain the raw mask values to the range $(0, 1)$:

$$\hat{\mathbf{m}} = \sigma(\mathbf{x}\mathbf{W}_m). \quad (5)$$

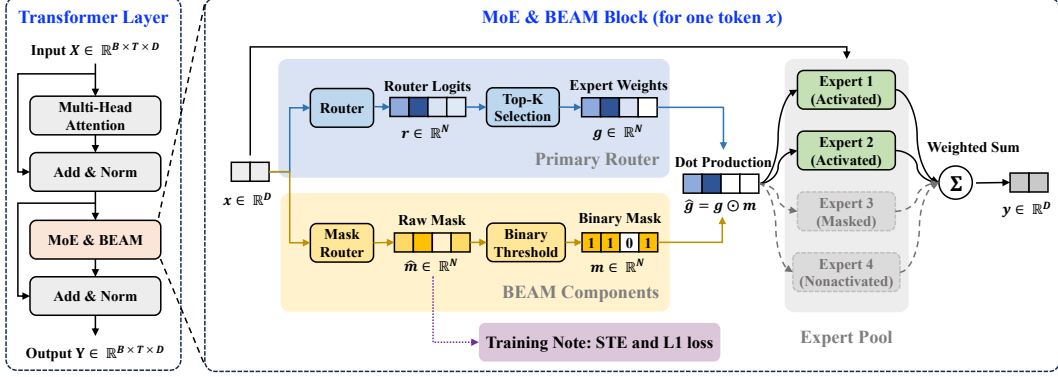


Figure 3: The illustration of our proposed BEAM method with 4 experts and $K=3$ as an example.

$\hat{\mathbf{m}}$ reflects the model’s confidence in the necessity of each expert for the current token.

Step 3: Binary Masking. We binarize the raw mask $\hat{\mathbf{m}}$ using a fixed threshold of $\tau = 0.5$ to obtain a discrete mask $\mathbf{m} \in \{0, 1\}^N$:

$$\mathbf{m}_i = \begin{cases} 1, & \text{if } \hat{\mathbf{m}}_i \geq 0.5, \\ 0, & \text{otherwise,} \end{cases} \quad (6)$$

Since $\mathbf{m}_i = 0$ disables expert i regardless of its Top-K status, the number of activated experts per token can be possibly reduced to 0.

Step 4: Masked Aggregation. The final routing weights $\hat{\mathbf{g}}$ are obtained by performing an element-wise multiplication between the Top-K weights \mathbf{g} and the binary mask \mathbf{m} :

$$\hat{\mathbf{g}} = \mathbf{g} \odot \mathbf{m}, \quad (7)$$

and the layer output is computed by aggregating the masked activations:

$$\mathbf{y} = \sum_{i=1}^N \hat{\mathbf{g}}_i \cdot \mathcal{E}_i(\mathbf{x}). \quad (8)$$

This design provides three key advantages. First, it decouples routing and sparsification, *i.e.*, the primary router handles expert selection and load balancing, while the mask router focuses exclusively on redundancy elimination, avoiding conflicting optimization objectives. Second, expert sparsity is learned end-to-end without manual tuning, enabling aggressive expert reduction while preserving model capability. Third, the binary mask provides a hardware-friendly signal that can be directly leveraged by custom CUDA kernels, facilitating efficient real-world deployment.

3.3 Training Strategy

BEAM is trained end-to-end using two key components. The first is the Straight-Through Estimator (STE) to handle the non-differentiable binarization operation. The second is an auxiliary sparsity regularization loss added to the standard MoE objective to jointly optimize task performance, expert load balancing, and computational efficiency.

3.3.1 Straight-Through Estimator

The binary mask \mathbf{m} is generated via a non-differentiable hard thresholding function as defined in Equation 6. To enable the mask router to be trained via backpropagation, we adopt the STE method [Bengio et al., 2013] to approximate the gradient. Specifically, during the backward pass, the threshold function is treated as an identity mapping, allowing the gradient of the loss \mathcal{L} with respect to \mathbf{m} to be propagated directly to the raw mask $\hat{\mathbf{m}}$:

$$\frac{\partial \mathcal{L}}{\partial \hat{\mathbf{m}}} \approx \frac{\partial \mathcal{L}}{\partial \mathbf{m}}. \quad (9)$$

This allows the mask router to be trained with backpropagation despite the discrete nature of \mathbf{m} . Note that all Top-K experts are computed regardless of \mathbf{m} to ensure proper gradient flow during training.

To ensure stable training, we initialize the mask router parameters to zero. This yields $\hat{\mathbf{m}} = 0.5$ and $\mathbf{m} = 1$ for all experts at the start of training, which preserves the original Top-K behavior and allows sparsity to emerge gradually as training proceeds.

3.3.2 Sparsity-Guided Optimization

The total training loss combines three terms. In addition to the standard language modeling loss \mathcal{L}_{lm} and the expert load-balancing loss \mathcal{L}_{bal} , we introduce an auxiliary sparsity regularization loss \mathcal{L}_{reg} , defined as the L_1 norm of the raw mask restricted to the Top-K candidate set \mathcal{T}_K :

$$\mathcal{L}_{reg} = \frac{1}{K} \sum_{i \in \mathcal{T}_K} |\hat{\mathbf{m}}_i|. \quad (10)$$

\mathcal{L}_{reg} directly encourages the mask router to suppress redundant experts among selected candidates without introducing extraneous gradients for non-selected experts.

The overall objective is a weighted sum:

$$\mathcal{L} = \mathcal{L}_{lm} + \alpha \mathcal{L}_{bal} + \beta \mathcal{L}_{reg}, \quad (11)$$

where α and β are hyperparameters that control the balance between expert utilization and computational efficiency. Through this sparsity-guided optimization, BEAM learns to activate only the necessary experts for each token, achieving high inference speed without compromising performance.

3.4 Theoretical Analysis

We provide a theoretical analysis of BEAM’s training dynamics. The core operation is the masked routing weight $\hat{\mathbf{g}} = \mathbf{g} \odot \mathbf{m}$, where \mathbf{g} is the output of the primary router and $\mathbf{m} = \mathbb{I}(\hat{\mathbf{m}} \geq 0.5)$ is the binary mask derived from $\hat{\mathbf{m}} = \sigma(\mathbf{a})$, with $\mathbf{a} = \mathbf{x}\mathbf{W}_m$ being the mask router pre-activation.

The mask router receives gradients from two sources: the task loss \mathcal{L}_{lm} propagated through the masked routing weights $\hat{\mathbf{g}}$ via STE, and the sparsity regularization \mathcal{L}_{reg} applied directly to the Top-K mask values. The load-balancing loss \mathcal{L}_{bal} is computed solely from the primary router’s weights \mathbf{g} before masking and does not produce gradients for the mask router.

Definition 3.1 (Gradient for Mask Router). Under STE, the full gradient of \mathcal{L} with respect to the mask router pre-activation \mathbf{a} is:

$$(\nabla_{\mathbf{a}} \mathcal{L})_i = \left(\frac{\partial \mathcal{L}_{lm}}{\partial \hat{g}_i} \cdot \mathbf{g}_i + \frac{\beta}{K} \cdot \mathbf{1}_{[i \in \mathcal{T}_K]} \right) \sigma'(a_i), \quad (12)$$

where \mathcal{T}_K denotes the Top-K candidate set and $\mathbf{1}_{[i \in \mathcal{T}_K]}$ is its indicator function.

Theorem 3.2 (Selective Gradient Propagation). *The gradient in Equation 12 satisfies:*

$$\mathbf{g}_i = 0 \quad \Rightarrow \quad (\nabla_{\mathbf{a}} \mathcal{L})_i = 0, \quad (13)$$

$$\mathbf{g}_i > 0 \quad \Rightarrow \quad (\nabla_{\mathbf{a}} \mathcal{L})_i = \left(\frac{\partial \mathcal{L}_{lm}}{\partial \hat{g}_i} \cdot \mathbf{g}_i + \frac{\beta}{K} \right) \sigma'(a_i). \quad (14)$$

Proof. Since $\hat{\mathbf{m}}_i = \sigma(a_i) \in (0, 1)$, the L1 gradient simplifies to $\partial|\hat{\mathbf{m}}_i|/\partial\hat{\mathbf{m}}_i = 1$. Note that $\sigma'(a_i) > 0$ for all $a_i \in \mathbb{R}$.

Case 1: If $\mathbf{g}_i = 0$, then $i \notin \mathcal{T}_K$. The task-loss term vanishes because $\mathbf{g}_i = 0$, and the regularization term vanishes because \mathcal{L}_{reg} is restricted to \mathcal{T}_K . Hence $(\nabla_{\mathbf{a}} \mathcal{L})_i = 0$, and the mask router receives no learning signal for non-selected experts.

Case 2: If $\mathbf{g}_i > 0$, then $i \in \mathcal{T}_K$ and both terms contribute. The gradient direction is determined by the sign of $\frac{\partial \mathcal{L}_{lm}}{\partial \hat{g}_i} \cdot \mathbf{g}_i + \frac{\beta}{K}$: the task-loss term drives a_i toward values that reduce \mathcal{L}_{lm} , while the constant $\frac{\beta}{K}$ consistently pushes a_i downward to encourage sparsity. Expert i is retained when its task contribution outweighs the sparsity pressure ($\frac{\partial \mathcal{L}_{lm}}{\partial \hat{g}_i} \cdot \mathbf{g}_i < -\frac{\beta}{K}$), and pruned otherwise. The hyperparameter β directly controls this trade-off. □

Further analysis of full expert masking behaviour and details of the efficient BEAM implementation in vLLM are provided in Appendix A.3 and Appendix A.4, respectively.

4 Experiments

4.1 Experimental Setup

Models and Training Data We evaluate BEAM on three representative MoE models: Qwen1.5-MoE-A2.7B [Bai et al., 2023], DeepSeekV2-Lite [Liu et al., 2024a], and Qwen3-30B-A3B [Yang et al., 2025a]. We conduct supervised fine-tuning using the Tulu 3 SFT Mixture Dataset [Lambert et al., 2024], which covers reasoning, coding, and general knowledge tasks. All baselines and BEAM are fine-tuned on the same dataset with identical training configurations to ensure fair comparison.

Baselines We compare against five methods: (1) **Top-K Reduced** trains with a smaller Top-K. (2) **Top-K Pruning** trains with the original Top-K and reduces Top-K at inference. (3) **MoE-Dynamic** [Huang et al., 2024] activates experts until cumulative routing probability exceeds threshold ϕ . (4) **AdaMoE** [Zeng et al., 2024] adds null experts with zero computation. (5) **DynMoE** [Guo et al., 2024] uses sigmoid router to adaptively determine activated experts.

Evaluation Benchmarks For accuracy evaluation, we use eight benchmarks from OpenCompass [Contributors, 2023] across three domains: Reasoning (Math [Hendrycks et al., 2021b], GSM8K [Cobbe et al., 2021]), HumanEval(H_Eval) [Chen et al., 2021]), Knowledge (MMLU [Hendrycks et al., 2021a], CEVAL [Huang et al., 2023], CMMLU [Li et al., 2023a]), and Common Sense (CommonsenseQA(CSQA) [Talmor et al., 2019], BoolQ [Clark et al., 2019]).

For acceleration evaluation, we report Time per Output Token (TPOT), Time to First Token (TTFT), and throughput under varying QPS using vLLM [Kwon et al., 2023]. All models run on a single NVIDIA H20 GPU with fixed input/output lengths of 128/32 tokens and 5000 test samples.

Hyperparameters For MoE-Dynamic, AdaMoE, and BEAM, we tune their respective hyperparameters, *i.e.*, cumulative probability threshold ϕ , null expert count, and L1 loss coefficient β , to match comparable sparsity levels with other methods at each setting. All experiments are conducted on NVIDIA H20 GPUs under identical hyperparameter settings, as detailed in Appendix B.1.

4.2 Performance Comparison

Table 1: Performance comparison on Qwen1.5-MoE-A2.7B under different sparsity levels. Best results within each sparsity group are marked in **bold**.

Methods/Tasks	Avg. K	Reasoning			Knowledge			CommonSense		Avg. (Acc. ↑)
		MATH	GSM8K	H_Eval	MMLU	CEVAL	CMMLU	BoolQ	CSQA	
Qwen1.5-MoE $K=4$	4.00	23.04	57.47	50.61	59.28	74.15	75.18	72.63	81.33	61.71
<i>Mid Sparsity</i>										
Top-K Pruning $K=2$	2.00	22.40	49.36	43.90	58.69	70.76	71.40	62.97	80.51	57.50
Top-K Reduced $K=2$	2.00	21.98	53.68	51.83	58.81	70.53	71.50	77.52	80.34	60.77
MoE-Dynamic $\phi=0.4$	2.20	20.94	51.86	47.56	57.85	67.35	67.84	73.82	80.34	58.45
AdaMoE $N_{\text{Null}}=60$	1.53	17.92	53.98	46.95	47.89	46.95	47.82	72.05	62.98	49.57
BEAM ($\beta=0.01$)	1.56	24.78	55.50	53.05	58.75	70.47	69.18	78.32	80.84	61.36
<i>High Sparsity</i>										
Top-K Pruning $K=1$	1.00	9.78	34.12	25.61	53.84	60.62	59.46	52.45	74.12	46.25
Top-K Reduced $K=1$	1.00	18.82	49.20	41.46	53.97	60.70	60.78	72.26	76.41	54.20
MoE-Dynamic $\phi=0.2$	1.47	17.22	45.64	42.07	53.29	58.46	58.85	74.25	74.61	53.05
AdaMoE $N_{\text{Null}}=120$	1.26	15.76	47.38	42.32	46.55	41.11	43.57	64.71	64.37	45.72
BEAM ($\beta=0.1$)	0.56	23.54	55.04	49.39	58.05	70.22	67.52	72.69	79.77	59.53
<i>Extreme Sparsity</i>										
BEAM ($\beta=1.0$)	0.11	18.72	51.18	42.07	54.17	58.97	57.15	69.11	69.94	52.66

Table 1, Table 2, and Table 3 summarize the performance and sparsity results of BEAM and baselines across multiple MoE models, organized by mid, high, and extreme sparsity levels. We report average activated experts per token (Avg-K) and downstream task scores. Comparisons with DynMoE are provided in Appendix B.3.

BEAM achieves extreme sparsity with minimal performance loss. BEAM consistently preserves over **98%** of original accuracy at mid sparsity across all three models while reducing Avg-K by 47%–61%. At high sparsity, Avg-K drops to as low as **14%** of the original (e.g., 0.56/4 on Qwen1.5) with over 95% accuracy retained. The advantage of BEAM is most evident under extreme sparsity. On DeepSeekV2, BEAM ($K = 0.48$) outperforms Top-K Reduced ($K = 1$) by **32.49%**, while on Qwen3 the margin reaches **33.29%**. On Qwen1.5, BEAM reaches Avg-K = 0.11, indicating that

Table 2: Performance comparison on Qwen3-30B-A3B under different sparsity levels. Best results within each sparsity group are marked in **bold**.

Methods \Tasks	Avg. K	Reasoning			Knowledge			CommonSense		Avg. (Acc. ↑)
		MATH	GSM8K	H_Eval	MMLU	CEVAL	CMMLU	BoolQ	CSQA	
Qwen3-30B-A3B $K=8$	8.00	58.28	88.02	82.93	81.80	83.56	83.69	86.76	86.24	81.41
<i>Mid Sparsity</i>										
Top-K Pruning $K=4$	4.00	48.76	49.51	76.83	73.49	75.85	76.27	81.04	75.02	69.60
Top-K Reduced $K=4$	4.00	56.44	84.46	80.49	78.27	80.40	78.27	87.68	85.18	78.90
MoE-Dynamic $\phi=0.3$	5.04	54.28	82.03	76.22	77.86	78.17	78.93	87.22	85.18	77.49
AdaMoE $N_{\text{Null}}=128$	4.02	41.68	62.44	69.93	72.51	62.71	63.39	84.71	77.15	66.81
BEAM ($\beta=0.01$)	4.23	55.16	85.52	81.71	80.09	81.46	81.53	88.07	86.40	79.99
<i>High Sparsity</i>										
Top-K Pruning $K=2$	2.00	0.68	1.14	0.00	25.39	17.51	16.42	17.31	16.87	11.92
Top-K Reduced $K=2$	2.00	44.60	77.79	72.56	72.99	72.63	72.99	83.85	80.02	72.18
MoE-Dynamic $\phi=0.1$	1.74	40.10	75.36	72.38	67.59	64.38	63.67	81.07	78.87	67.93
AdaMoE $N_{\text{Null}}=256$	2.64	34.06	73.01	58.54	44.50	38.75	37.76	61.04	60.44	51.01
BEAM ($\beta=0.1$)	1.23	55.44	85.90	81.10	76.06	74.04	74.54	85.75	84.28	77.14
<i>Extreme Sparsity</i>										
Top-K Reduced $K=1$	1.00	27.96	63.08	51.22	58.26	52.97	53.05	56.21	68.88	53.95
BEAM ($\beta=1.0$)	0.56	52.20	81.96	77.44	69.44	66.28	69.36	78.47	80.10	71.91

Table 3: Performance comparison on DeepSeekV2-Lite under different sparsity levels. Best results within each sparsity group are marked in **bold**.

Methods \Tasks	Avg. K	Reasoning			Knowledge			CommonSense		Avg. (Acc. ↑)
		MATH	GSM8K	H_Eval	MMLU	CEVAL	CMMLU	BoolQ	CSQA	
DeepSeekV2-Lite $K=6$	6.00	20.02	62.70	43.90	55.04	55.26	60.93	75.20	68.14	55.15
<i>Mid Sparsity</i>										
Top-K Pruning $K=4$	4.00	15.10	57.09	37.80	46.68	53.25	60.00	69.69	67.40	50.88
Top-K Reduced $K=4$	4.00	16.58	57.24	40.85	54.70	55.89	60.40	76.39	72.48	54.32
MoE-Dynamic $\phi=0.3$	4.31	19.08	35.63	38.35	42.95	53.36	58.12	63.55	70.60	47.70
AdaMoE $N_{\text{Null}}=64$	3.25	12.00	37.76	25.67	53.01	57.28	58.85	62.32	69.86	47.09
BEAM ($\beta=0.01$)	2.61	20.36	60.27	46.95	56.65	54.12	60.42	76.57	65.11	55.06
<i>High Sparsity</i>										
Top-K Pruning $K=2$	2.00	13.38	46.02	28.66	43.25	51.06	36.91	58.90	58.64	42.10
Top-K Reduced $K=2$	2.00	15.18	51.10	34.76	51.65	53.35	60.39	68.87	66.83	50.27
MoE-Dynamic $\phi=0.1$	3.90	15.96	56.56	39.00	28.52	55.10	58.43	34.56	71.09	44.90
AdaMoE $N_{\text{Null}}=128$	2.11	9.24	28.96	20.73	39.70	54.83	52.29	54.50	70.27	41.31
BEAM ($\beta=0.1$)	1.08	17.18	59.21	43.29	48.08	56.15	60.67	71.07	70.93	53.32
<i>Extreme Sparsity</i>										
Top-K Reduced $K=1$	1.00	7.90	31.99	25.00	28.75	41.46	45.01	53.14	52.91	35.77
BEAM ($\beta=1.0$)	0.48	11.72	45.19	42.07	38.33	50.11	54.48	69.66	67.57	47.39

most tokens completely bypass routed experts, while still retaining 85% of the original performance, which demonstrates effective token-adaptive redundancy removal.

Existing dynamic routing methods underperform in post-training settings. Top-K Pruning degrades sharply at higher sparsity, while Top-K Reduced is more stable but its fixed per-token budget consistently underperforms BEAM. Even at extreme sparsity, BEAM with fewer average experts outperforms Top-K Reduced ($K = 1$) on both Qwen3 and DeepSeek. MoE-Dynamic and AdaMoE also fall short: the former requires model-specific threshold tuning without competitive trade-offs, while the latter suffers from performance degradation due to null-expert interference. BEAM avoids these issues by decoupling sparsification from expert selection via a lightweight mask router, enabling stable training and preserving the original expert load balance (Appendix B.5).

β **provides smooth control over the sparsity-accuracy trade-off.** Increasing β consistently improves sparsity with gradual accuracy loss (Tables 1–3), making it straightforward to adapt the method to deployment constraints via a single parameter. At $\beta = 0.1$, BEAM preserves over 95% accuracy across all models, offering a good trade-off.

4.3 Acceleration Comparison

We evaluate inference acceleration under both online and offline settings. In the online setting, models are deployed as services and we measure TTFT and TPOT across varying QPS to simulate real-world serving. In the offline setting, we use a large fixed batch size to maximize GPU utilization and report

throughput, reflecting scenarios like large-scale LLM knowledge distillation. For fair comparison with performance-efficiency tradeoff, we tested the inference speed of all baseline methods and BEAM under *High Sparsity*.

As shown in Figure 4, BEAM achieves consistent speedups across all models and settings. It achieves at least $1.3\times$ improvement in TPOT and over $1.1\times$ gains in both TTFT and throughput. Notably, on DeepSeek-V2-Lite at QPS=24, BEAM reaches up to $2.5\times$ decoding acceleration. The achievable speedup is limited by model architecture. For example, Qwen1.5-MoE-A2.7B contains 4 shared experts out of 8 total, limiting their MoE layer FLOPs reduction to at most 50%. In contrast, Qwen3-30B-A3B has no shared experts, enabling an 85% FLOPs reduction and substantially higher throughput gains. In comparison, MoE-Dynamic and AdaMoE achieve limited sparsity and introduce extra overhead, yielding negligible or no acceleration benefits.

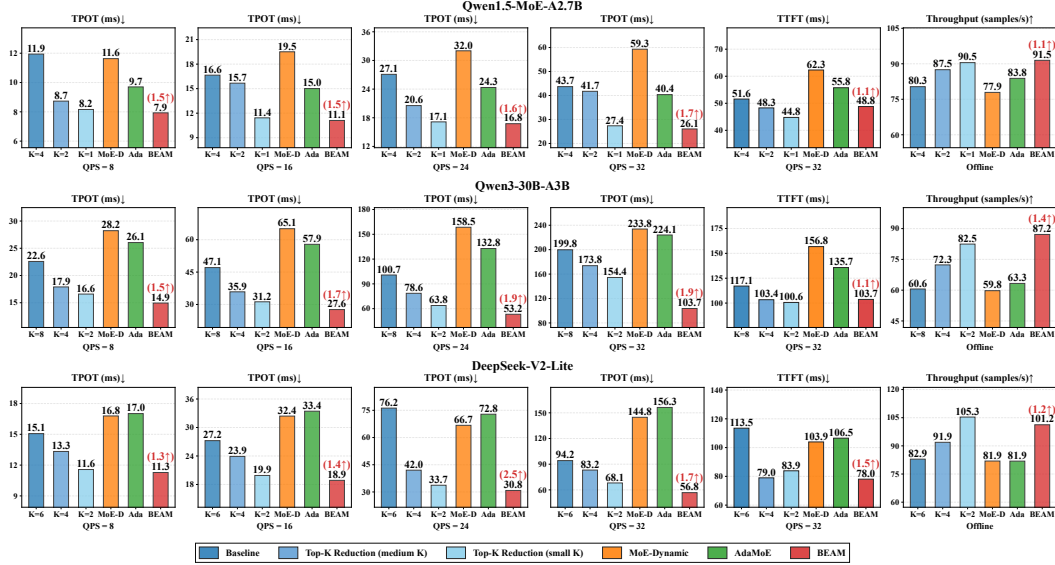


Figure 4: Comparison of TPOT, TTFT, and throughput across different methods.

4.4 Ablation Study

Table 4: Binary threshold τ ablation on Qwen1.5.

Threshold	Avg. K	Reason.	Know.	Common.	Avg. \uparrow
$\tau = 0.1$	0.78	43.91	66.80	66.43	58.12
$\tau = 0.3$	0.70	44.41	66.37	70.82	59.25
$\tau = 0.5$	0.56	43.01	65.12	76.23	59.61
$\tau = 0.7$	0.42	41.92	62.23	69.72	56.49
$\tau = 0.9$	0.28	41.09	60.00	59.26	52.72

Table 5: Training configuration ablation on Qwen3.

Configs.	Avg. K	Reason.	Know.	Common.	Avg. \uparrow
BEAM	1.23	74.15	74.88	85.02	77.14
- w/o. \mathcal{L}_{reg}	6.31	75.42	76.55	83.23	77.80 (0.9% \uparrow)
- \mathcal{L}_1 to \mathcal{L}_2	2.01	71.34	73.21	84.29	75.28 (2.4% \downarrow)
- Soft	1.34	12.70	21.94	42.30	23.56 (69.5% \downarrow)
- Soft w/ Temp.	1.78	65.30	72.35	82.29	73.31 (5.0% \downarrow)

Ablation on Binary Threshold We evaluate binarization thresholds $\tau \in \{0.1, 0.3, 0.5, 0.7, 0.9\}$ on Qwen1.5-MoE-A2.7B, as shown in Table 4. Increasing τ monotonically reduces Avg-K and thus increases sparsity. We find that $\tau = 0.5$ achieves the best overall performance, largely driven by stronger commonsense results. A plausible explanation is that $\tau = 0.5$ offers the greatest gradient sensitivity around the decision boundary while maintaining a stable Top-K initialization. Based on this result, we fix $\tau = 0.5$ and vary only the regularization coefficient β to control sparsity.

Ablation on Training Approach We evaluate several training variants on Qwen3-30B-A3B, including removing \mathcal{L}_{reg} , replacing L1 with L2 regularization, and replacing STE-based binary masking with soft-mask training. For the latter, we consider both plain sigmoid gating (Soft) and a temperature-scaled sigmoid that gradually sharpens the mask (Soft w/ Temp.). As shown in Table 5, removing \mathcal{L}_{reg} slightly improves reasoning performance but substantially increases expert activation. L2 regularization is inferior to L1 in both sparsity and accuracy. Both soft-mask variants also underperform binary-mask training, where plain sigmoid gating fails severely because of the train-inference mismatch, while temperature scaling only partially mitigates this issue. Overall, the results support the use of \mathcal{L}_{reg} , L1 regularization, and STE-based binary masking in BEAM.

5 Analysis

5.1 Token-wise Sparsity Analysis

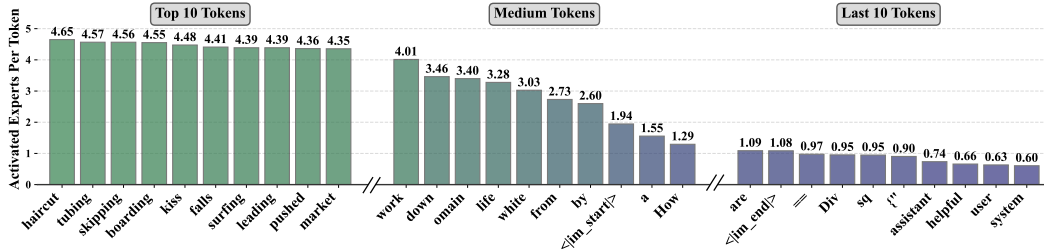
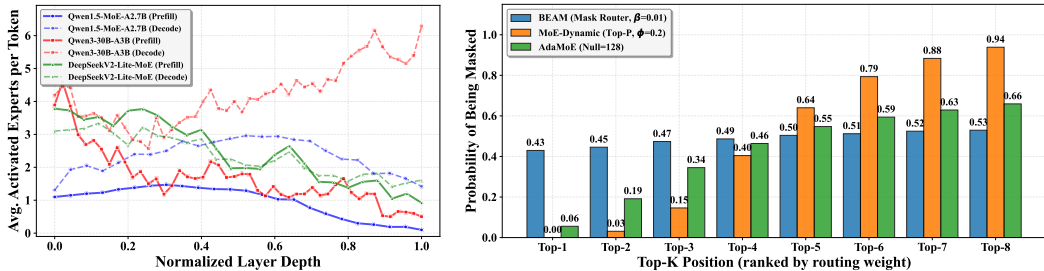


Figure 5: The average number of activated experts per token in BEAM: Qwen3-30B-A3B.

To understand how BEAM adapts computation per token, we visualize the average number of activated experts across tokens, as shown in Figure 5. We obtain several key findings. **1. Expert activation varies across tokens.** The most demanding tokens activate up to 4.65 experts on average, versus only 0.6 for the least demanding. **2. Activation aligns with semantic richness.** Content words (e.g., nouns, verbs) consistently trigger more experts than function words (e.g., prepositions) and punctuation. **3. Chat template tokens are highly redundant.** Fixed prompts like “You are a helpful assistant” activate few experts yet maintain performance, suggesting minimal informational value. These findings show that BEAM dynamically allocates computation based on token informativeness.

5.2 Layer-wise and Position-wise Analysis



(a) Layer-wise activated experts.

(b) Position-wise masking probability.

Figure 6: Layer-wise sparsity and position-wise masking analysis.

We measure the average number of activated experts per layer during prefill and decode on 1,000 randomly sampled inputs (Figure 6a). DeepSeek exhibits nearly identical expert usage in both phases, while Qwen1.5 and Qwen3 consistently use more experts during decoding. These models also develop an encoder-decoder-like pattern: shallower layers primarily support knowledge storage, while deeper layers allocate more expert capacity to decoding and reasoning, meaning that BEAM adapts layer-wise sparsity to functional roles. We further compare the per-position masking probability of BEAM, MoE-Dynamic, and AdaMoE on Qwen3 Under similar sparsity conditions. (Figure 6b). MoE-Dynamic exhibits strong position bias, never masking Top-1 (0.00) and applying extremely high masking beyond Top-6 (0.79~0.94). AdaMoE shows a monotonic increase from Top-1 (0.06) to Top-8 (0.66), indicating moderate but still rank-dependent bias. In contrast, BEAM shows only a mild increase from Top-1 (0.43) to Top-8 (0.53), demonstrating that it evaluates expert relevance based on token-specific features rather than routing rank. Another layer-wise rank masking analysis is provided in Appendix B.4.

We also provide task-specific acceleration analysis, expert load balancing analysis, and token-layer sparsity visualizations. Details can be found in Appendix B.6, B.5, and B.7.

6 Conclusion

We propose BEAM, a plug-and-play dynamic routing framework that introduces a lightweight mask router to selectively deactivate redundant experts within the Top-K set, enabling token-adaptive sparsity without modifying the model architecture. Integrated into vLLM via an efficient CUDA kernel, BEAM delivers up to $2.5\times$ faster decoding and $1.4\times$ higher throughput with over 98% accuracy retention, demonstrating that decoupling sparsity control from routing enables stable and practical MoE inference acceleration.

References

- Maryam Akhavan Aghdam, Hongpeng Jin, and Yanzhao Wu. Da-moe: Towards dynamic expert allocation for mixture-of-experts models. *arXiv preprint arXiv:2409.06669*, 2024.
- Walaa Amer, Fadi Kurdahi, et al. Conflayers: Adaptive confidence-based layer skipping for self-speculative decoding. *arXiv preprint arXiv:2604.14612*, 2026.
- Jinze Bai, Shuai Bai, Yunfei Chu, Zeyu Cui, Kai Dang, Xiaodong Deng, Yang Fan, Wenbin Ge, Yu Han, Fei Huang, et al. Qwen technical report. *arXiv preprint arXiv:2309.16609*, 2023.
- Yoshua Bengio, Nicholas Léonard, and Aaron Courville. Estimating or propagating gradients through stochastic neurons for conditional computation. *arXiv preprint arXiv:1308.3432*, 2013.
- I-Chun Chen, Hsu-Shen Liu, Wei-Fang Sun, Chen-Hao Chao, Yen-Chang Hsu, and Chun-Yi Lee. Retraining-free merging of sparse moe via hierarchical clustering. In *Forty-second International Conference on Machine Learning*, 2025. URL <https://openreview.net/forum?id=hs10zRxzXL>.
- Mark Chen, Jerry Tworek, Heewoo Jun, Qiming Yuan, Henrique Ponde de Oliveira Pinto, Jared Kaplan, Harri Edwards, Yuri Burda, Nicholas Joseph, Greg Brockman, Alex Ray, Raul Puri, Gretchen Krueger, Michael Petrov, Heidy Khlaaf, Girish Sastry, Pamela Mishkin, Brooke Chan, Scott Gray, Nick Ryder, Mikhail Pavlov, Alethea Power, Lukasz Kaiser, Mohammad Bavarian, Clemens Winter, Philippe Tillet, Felipe Petroski Such, Dave Cummings, Matthias Plappert, Fotios Chantzis, Elizabeth Barnes, Ariel Herbert-Voss, William Hebgen Guss, Alex Nichol, Alex Paino, Nikolas Tezak, Jie Tang, Igor Babuschkin, Suchir Balaji, Shantanu Jain, William Saunders, Christopher Hesse, Andrew N. Carr, Jan Leike, Josh Achiam, Vedant Misra, Evan Morikawa, Alec Radford, Matthew Knight, Miles Brundage, Mira Murati, Katie Mayer, Peter Welinder, Bob McGrew, Dario Amodei, Sam McCandlish, Ilya Sutskever, and Wojciech Zaremba. Evaluating large language models trained on code, 2021.
- Christopher Clark, Kenton Lee, Ming-Wei Chang, Tom Kwiatkowski, Michael Collins, and Kristina Toutanova. BoolQ: Exploring the surprising difficulty of natural yes/no questions. In Jill Burstein, Christy Doran, and Tamar Solorio, editors, *Proceedings of the 2019 Conference of the North American Chapter of the Association for Computational Linguistics: Human Language Technologies, Volume 1 (Long and Short Papers)*, pages 2924–2936, Minneapolis, Minnesota, June 2019. Association for Computational Linguistics. doi: 10.18653/v1/N19-1300. URL <https://aclanthology.org/N19-1300/>.
- Karl Cobbe, Vineet Kosaraju, Mohammad Bavarian, Mark Chen, Heewoo Jun, Lukasz Kaiser, Matthias Plappert, Jerry Tworek, Jacob Hilton, Reiichiro Nakano, Christopher Hesse, and John Schulman. Training verifiers to solve math word problems. *arXiv preprint arXiv:2110.14168*, 2021.
- OpenCompass Contributors. Opencompass: A universal evaluation platform for foundation models. <https://github.com/open-compass/opencompass>, 2023.
- Anchun Gui, Bei Li, Bingyang Tao, Bole Zhou, Borun Chen, Chao Zhang, Chengcheng Han, Chenhui Yang, Chi Zhang, et al. Introducing longcat-flash-thinking: A technical report. *arXiv preprint arXiv:2509.18883*, 2025.
- Yongxin Guo, Zhenglin Cheng, Xiaoying Tang, Zhaopeng Tu, and Tao Lin. Dynamic mixture of experts: An auto-tuning approach for efficient transformer models. *arXiv preprint arXiv:2405.14297*, 2024.
- Dan Hendrycks, Collin Burns, Steven Basart, Andy Zou, Mantas Mazeika, Dawn Song, and Jacob Steinhardt. Measuring massive multitask language understanding. *Proceedings of the International Conference on Learning Representations (ICLR)*, 2021a.
- Dan Hendrycks, Collin Burns, Saurav Kadavath, Akul Arora, Steven Basart, Eric Tang, Dawn Song, and Jacob Steinhardt. Measuring mathematical problem solving with the math dataset. *NeurIPS*, 2021b.

- Quzhe Huang, Zhenwei An, Nan Zhuang, Mingxu Tao, Chen Zhang, Yang Jin, Kun Xu, Liwei Chen, Songfang Huang, and Yansong Feng. Harder tasks need more experts: Dynamic routing in moe models. *arXiv preprint arXiv:2403.07652*, 2024.
- Yuzhen Huang, Yuzhuo Bai, Zhihao Zhu, Junlei Zhang, Jinghan Zhang, Tangjun Su, Junteng Liu, Chuancheng Lv, Yikai Zhang, Jiayi Lei, Yao Fu, Maosong Sun, and Junxian He. C-eval: A multi-level multi-discipline chinese evaluation suite for foundation models. In *Advances in Neural Information Processing Systems*, 2023.
- Albert Q Jiang, Alexandre Sablayrolles, Antoine Roux, Arthur Mensch, Blanche Savary, Chris Bamford, Devendra Singh Chaplot, Diego de las Casas, Emma Bou Hanna, Florian Bressand, et al. Mixtral of experts. *arXiv preprint arXiv:2401.04088*, 2024.
- Can Jin, Hongwu Peng, Mingcan Xiang, Qixin Zhang, Xiangchi Yuan, Amit Hasan, Ohiremen Dibua, Yifan Gong, Yan Kang, and Dimitris N Metaxas. Sparsity-controllable dynamic top-p moe for large foundation model pre-training. *arXiv preprint arXiv:2512.13996*, 2025.
- Peng Jin, Bo Zhu, Li Yuan, and Shuicheng Yan. Moe++: Accelerating mixture-of-experts methods with zero-computation experts. *arXiv preprint arXiv:2410.07348*, 2024.
- Woosuk Kwon, Zhuohan Li, Siyuan Zhuang, Ying Sheng, Lianmin Zheng, Cody Hao Yu, Joseph E. Gonzalez, Hao Zhang, and Ion Stoica. Efficient memory management for large language model serving with pagedattention. In *Proceedings of the ACM SIGOPS 29th Symposium on Operating Systems Principles*, 2023.
- Nathan Lambert, Jacob Morrison, Valentina Pyatkin, Shengyi Huang, Hamish Ivison, Faeze Brahman, Lester James V Miranda, Alisa Liu, Nouha Dziri, Shane Lyu, et al. Tulu 3: Pushing frontiers in open language model post-training. *arXiv preprint arXiv:2411.15124*, 2024.
- Tim Lawson and Laurence Aitchison. Learning to skip the middle layers of transformers. *arXiv preprint arXiv:2506.21103*, 2025.
- Dmitry Lepikhin, HyoukJoong Lee, Yuanzhong Xu, Dehao Chen, Orhan Firat, Yanping Huang, Maxim Krikun, Noam Shazeer, and Zhifeng Chen. Gshard: Scaling giant models with conditional computation and automatic sharding. *arXiv preprint arXiv:2006.16668*, 2020.
- Haonan Li, Yixuan Zhang, Fajri Koto, Yifei Yang, Hai Zhao, Yeyun Gong, Nan Duan, and Timothy Baldwin. Cmmlu: Measuring massive multitask language understanding in chinese, 2023a.
- Jiamin Li, Qiang Su, Yitao Yang, Yimin Jiang, Cong Wang, and Hong Xu. Adaptive gating in mixture-of-experts based language models. *arXiv preprint arXiv:2310.07188*, 2023b.
- Pingzhi Li, Zhenyu Zhang, Prateek Yadav, Yi-Lin Sung, Yu Cheng, Mohit Bansal, and Tianlong Chen. Merge, then compress: Demystify efficient smoe with hints from its routing policy. *arXiv preprint arXiv:2310.01334*, 2023c.
- Aixin Liu, Bei Feng, Bin Wang, Bingxuan Wang, Bo Liu, Chenggang Zhao, Chengqi Deng, Chong Ruan, Damai Dai, Daya Guo, et al. Deepseek-v2: A strong, economical, and efficient mixture-of-experts language model. *arXiv preprint arXiv:2405.04434*, 2024a.
- Enshu Liu, Junyi Zhu, Zinan Lin, Xuefei Ning, Matthew B Blaschko, Shengen Yan, Guohao Dai, Huazhong Yang, and Yu Wang. Efficient expert pruning for sparse mixture-of-experts language models: Enhancing performance and reducing inference costs. *arXiv preprint arXiv:2407.00945*, 2024b.
- Xudong Lu, Qi Liu, Yuhui Xu, Aojun Zhou, Siyuan Huang, Bo Zhang, Junchi Yan, and Hongsheng Li. Not all experts are equal: Efficient expert pruning and skipping for mixture-of-experts large language models. In Lun-Wei Ku, Andre Martins, and Vivek Srikumar, editors, *Proceedings of the 62nd Annual Meeting of the Association for Computational Linguistics (Volume 1: Long Papers)*, pages 6159–6172, Bangkok, Thailand, August 2024. Association for Computational Linguistics. doi: 10.18653/v1/2024.acl-long.334. URL <https://aclanthology.org/2024.acl-long.334/>.

- Noam Shazeer, Azalia Mirhoseini, Krzysztof Maziarz, Andy Davis, Quoc Le, Geoffrey Hinton, and Jeff Dean. Outrageously large neural networks: The sparsely-gated mixture-of-experts layer. *arXiv preprint arXiv:1701.06538*, 2017.
- Zhenpeng Su, Zijia Lin, Xue Bai, Xing Wu, Yizhe Xiong, Haoran Lian, Guangyuan Ma, Hui Chen, Guiguang Ding, Wei Zhou, et al. Maskmoe: Boosting token-level learning via routing mask in mixture-of-experts. *arXiv preprint arXiv:2407.09816*, 2024.
- Alon Talmor, Jonathan Herzig, Nicholas Lourie, and Jonathan Berant. CommonsenseQA: A question answering challenge targeting commonsense knowledge. In *Proceedings of the 2019 Conference of the North American Chapter of the Association for Computational Linguistics: Human Language Technologies, Volume 1 (Long and Short Papers)*, pages 4149–4158, Minneapolis, Minnesota, June 2019. Association for Computational Linguistics. doi: 10.18653/v1/N19-1421. URL <https://aclanthology.org/N19-1421>.
- An Yang, Anfeng Li, Baosong Yang, Beichen Zhang, Binyuan Hui, Bo Zheng, Bowen Yu, Chang Gao, Chengen Huang, Chenxu Lv, et al. Qwen3 technical report. *arXiv preprint arXiv:2505.09388*, 2025a.
- Cheng Yang, Yang Sui, Jinqi Xiao, Lingyi Huang, Yu Gong, Yuanlin Duan, Wenqi Jia, Miao Yin, Yu Cheng, and Bo Yuan. Moe-i2: Compressing mixture of experts models through inter-expert pruning and intra-expert low-rank decomposition. *arXiv preprint arXiv:2411.01016*, 2024a.
- Ning Yang, Fangxin Liu, Junjie Wang, Tao Yang, Kan Liu, Haibing Guan, and Li Jiang. Dash: Input-aware dynamic layer skipping for efficient llm inference with markov decision policies. *arXiv preprint arXiv:2505.17420*, 2025b.
- Yuanhang Yang, Shiyi Qi, Wenchao Gu, Chaozheng Wang, Cuiyun Gao, and Zenglin Xu. Xmoe: Sparse models with fine-grained and adaptive expert selection. *arXiv preprint arXiv:2403.18926*, 2024b.
- Zihao Zeng, Yibo Miao, Hongcheng Gao, Hao Zhang, and Zhijie Deng. Adamoe: Token-adaptive routing with null experts for mixture-of-experts language models. *arXiv preprint arXiv:2406.13233*, 2024.
- Zeliang Zhang, Xiaodong Liu, Hao Cheng, Chenliang Xu, and Jianfeng Gao. Diversifying the expert knowledge for task-agnostic pruning in sparse mixture-of-experts. In *Findings of the Association for Computational Linguistics: ACL 2025*, pages 86–102, 2025.

A Appendix on Method

A.1 Impact Statements

This work focuses on improving the computational efficiency of Mixture-of-Experts models. We do not identify any societal impacts specific to the proposed method beyond those already associated with the general use and deployment of large language models.

A.2 Limitations

Our work has several limitations. First, BEAM is evaluated on three MoE architectures; its effectiveness on other MoE designs (e.g., with different gating mechanisms or expert granularities) remains to be validated. Second, BEAM requires a post-training SFT phase to learn the mask router, which incurs additional training cost proportional to the model size. Third, the achievable inference speedup depends on the model’s shared-expert ratio. For example, architectures with a large proportion of shared experts may benefit less, as shared-expert computation cannot be reduced by BEAM. Finally, our acceleration benchmarks are conducted on single-GPU settings, and the interaction between BEAM’s dynamic sparsity and multi-GPU expert parallelism strategies needs further investigation.

A.3 Behaviors under Zero Activation

Since BEAM permits between 0 and K activated experts, the zero-activation case requires special consideration. In a modern Transformer MoE block, the hidden state update follows:

$$\mathbf{h}' = \mathbf{h} + \sum_{i=1}^N \hat{\mathbf{g}}_i \mathcal{E}_i(\mathcal{N}(\mathbf{h})) + \delta_{\text{sh}} \mathbf{g}_{\text{sh}} \mathcal{E}_{\text{sh}}(\mathcal{N}(\mathbf{h})), \quad (15)$$

where $\mathcal{N}(\cdot)$ denotes the normalization function, $\mathcal{E}_i(\cdot)$ denotes the i -th routed expert, $\hat{\mathbf{g}}_i \in \mathbb{R}$ denotes the normalized routing weight assigned to expert i , $\mathcal{E}_{\text{sh}}(\cdot)$ denotes the shared expert, \mathbf{g}_{sh} denotes the routing weight assigned to the shared expert, and $\delta_{\text{sh}} \in \{0, 1\}$ is an indicator variable specifying whether a shared expert is present. When all routed experts are skipped, *i.e.*, $\hat{\mathbf{g}}_i = 0$ for all $i \in \{1, \dots, N\}$, then the update becomes:

$$\mathbf{h}' = \mathbf{h} + \delta_{\text{sh}} \mathbf{g}_{\text{sh}} \mathcal{E}_{\text{sh}}(\mathcal{N}(\mathbf{h})). \quad (16)$$

Therefore, if $\delta_{\text{sh}} = 1$, as in architectures with shared experts such as Qwen1.5-MoE and DeepSeek, the layer reduces to shared-expert-only computation. If $\delta_{\text{sh}} = 0$, as in architectures without shared experts such as Qwen3-MoE, the token bypasses the entire MoE layer through the residual path.

Under zero activation, BEAM degenerates into a form of dynamic layer skipping, which has also been studied in prior work as an efficient inference acceleration mechanism [Yang et al., 2025b, Lawson and Aitchison, 2025, Amer et al., 2026]. Empirically, as shown in Section 4.2, BEAM maintains strong model performance even when the average number of activated experts is below 1, implying that zero-activation cases occur frequently in practice. This observation suggests that substantial layer computation in LLMs is redundant. Moreover, the analysis in Section 5 shows that zero activation arises more often in deeper layers during prefill and for tokens with limited semantic content.

A.4 Key Modifications for BEAM

We implement BEAM in vLLM by minimally extending its standard MoE CUDA pipeline with two kernel-level changes. First, `mask_route_kernel` writes the expert index as -1 whenever the corresponding mask logit is non-positive. Second, `moe_align_block_size_kernel` ignores all -1 entries during expert-wise token grouping and block alignment, thereby removing masked experts from subsequent computation. This modification is lightweight, preserves compatibility with vLLM’s existing optimizations such as operator fusion and memory coalescing, and introduces negligible integration overhead. The core code is provided below, and the full implementation will be released upon acceptance.

```
1  template<typename scalar_t>
2  __global__ void mask_route_kernel(
3  const int64_t* __restrict__ topk_ids,           // Input: Top-K expert
indices
```

```

4     const scalar_t* __restrict__ mask_logits,    // Input: Expert mask
logits
5     int64_t* __restrict__ output_ids,          // Output: Masked expert
IDs
6     const int num_tokens, const int top_k, const int num_experts) {
7
8     int idx = blockIdx.x * blockDim.x + threadIdx.x;
9     if (idx >= num_tokens * top_k) return;
10    int token_idx = idx / top_k;
11    int slot_idx = idx % top_k;
12    int input_idx = token_idx * top_k + slot_idx;
13    int64_t original_expert = topk_ids[input_idx];
14
15    if (token_idx >= num_tokens || slot_idx >= top_k ||
16        original_expert < 0 || original_expert >= num_experts) {
17        output_ids[input_idx] = -1;
18        return;
19    }
20
21    // Apply binary mask: keep if mask_logits > 0, else set to -1
22    int expert_idx = token_idx * num_experts + original_expert;
23    scalar_t logit = mask_logits[expert_idx];
24    output_ids[input_idx] = (logit > 0) ? original_expert : -1;
25 }
26
27 template <typename scalar_t, typename token_cnts_t>
28 __global__ void moe_align_block_size_kernel(/* ... */) {
29     // ... thread setup ...
30     for (int i = start_idx; i < end_idx; ++i) {
31         int64_t expert_id = topk_ids[i];
32         if (expert_id != -1) { // Skip masked experts
33             ++tokens_cnts[index(num_experts, threadIdx.x + 1, expert_id)
34         }
35     }
36     // ... rest of alignment logic ...
37 }

```

B Appendix on Experiment

B.1 Experimental Setup

B.1.1 Models

We do experiments on three representative MoE models: Qwen1.5-MoE-A2.7B [Bai et al., 2023], DeepSeekV2-Lite [Liu et al., 2024a], and Qwen3-30B-A3B [Yang et al., 2025a].

- **Qwen1.5-MoE-A2.7B:** Each token activates 4 shared experts and 4 routed experts (out of 60) in each layer.
- **DeepSeekV2-Lite:** Each token activates 2 shared experts and 6 routed experts (out of 64) in each layer.
- **Qwen3-30B-A3B:** Each token activates 8 routed experts (out of 128) in each layer.

More details can be found in Table 6.

B.1.2 Hyper-Parameters

Tables 6 summarize the main configurations for all MoE models studied in this work. All trainings and evaluations are performed on NVIDIA H20 GPUs

B.1.3 Benchmarks

For accuracy comparison, we select a diverse set of tasks from the OpenCompass [Contributors, 2023] benchmark, covering multiple domains: Reasoning (MATH [Hendrycks et al., 2021b],

Table 6: Main hyperparameters for each model.

Model Config	Qwen1.5-MoE-A2.7B	DeepSeekV2-Lite	Qwen3-30B-A3B
Total Params (B)	14.3	16	30
Activated Params (B)	2.7	2.4	3
MoE Layers / Total Layers	24/24	26/27	48/48
Experts per MoE Layer	60	64	128
Activated Experts per Token	4 (selected) + 4 (shared)	6 (selected) + 2 (shared)	8
hidden size	2560	2048	2048
intermediate size	5632	10944	6144
Vocabulary Size	151936	102400	151936
Inference Setting	Qwen1.5-MoE-A2.7B	DeepSeekV2-Lite	Qwen3-30B-A3B
Temperature	0.7	0.3	0.7
Top- p	0.8	0.95	0.8
Top- k	20	50	20
Repetition Penalty	1.05	1.00	1.00
Max Output Tokens	1024	1024	2048
Batch Size	16	16	16
Training Setting	Qwen1.5-MoE-A2.7B	DeepSeekV2-Lite	Qwen3-30B-A3B
Learning Rate	5×10^{-5}	5×10^{-5}	5×10^{-5}
Learning Rate Schedule	Linear	Linear	Linear
Load Balancing Loss Coefficient (α)	1×10^{-3}	1×10^{-3}	1×10^{-3}
Per Device Batch Size	32	32	32
Number of GPUs	32	32	64
Max Token Length	4096	4096	4096
Warm up ratio	0.03	0.03	0.03
Number of Epochs	2	2	2

GSM8K [Cobbe et al., 2021], and Human Eval [Chen et al., 2021]); Knowledge (MMLU [Hendrycks et al., 2021a], CEVAL [Huang et al., 2023], and CMMLU [Li et al., 2023a]); and CommonSense (CommonsenseQA [Talmor et al., 2019], BoolQ [Clark et al., 2019]). Details and examples of these tasks are provided in Table 7.

For acceleration comparison, we use vLLM [Kwon et al., 2023] as the inference framework. Each model is deployed on a single GPU, and we record the *Time per Output Token* (TPOT, in ms) across different *Queries per Second* (QPS), the *Time To First Token* (TTFT, in ms) in 32 QPS (high-computing scenarios), and the offline *Throughput* (samples/s). The input and output sequence lengths are fixed at 128 and 32 tokens, respectively, and each test processes a total of 5,000 samples.

B.2 Training Dynamics

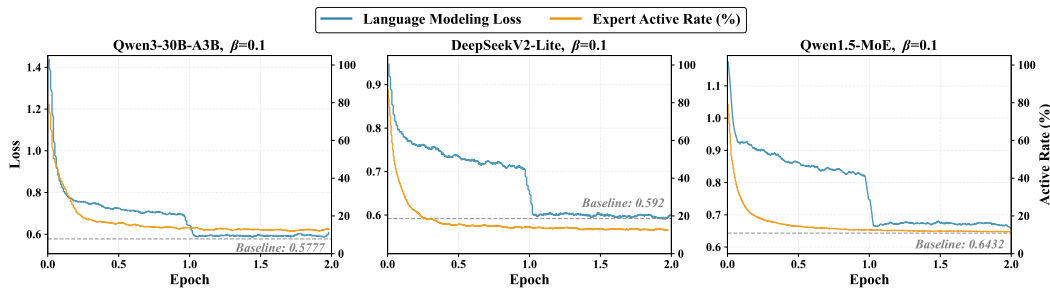


Figure 7: Training curves of BEAM ($\beta = 0.1$) on three MoEs. Blue: language modeling loss (left axis). Orange: expert active rate (right axis). Gray dashed line: SFT baseline loss without BEAM.

Figure 7 shows the language modeling loss and expert active rate during BEAM training ($\beta = 0.1$) on all three models. The gray dashed line indicates the converged loss of standard SFT without BEAM. Two observations emerge. First, BEAM’s language modeling loss converges to a level comparable to the SFT baseline across all models, confirming that the mask router and sparsity regularization do not compromise model capacity. Second, expert sparsification concentrates in the first ~ 0.5 epoch, where

Table 7: Overview of OpenCompass tasks used for evaluation.

Task	Domain/Format	Description / Example
Math [Hendrycks et al., 2021b]	Reasoning / Open-Ended	A dataset of high school-level mathematical problems requiring step-by-step solutions. <i>Example:</i> A positive multiple of 45 less than 1000 is randomly selected. What is the probability that it is a two-digit integer? Express your answer as a common fraction.
GSM8K [Cobbe et al., 2021]	Reasoning / Open-Ended	Grade school math word problems with a focus on multi-step reasoning. <i>Example:</i> Shiloh is 44 years old today. In 7 years, he will be three times as old as his nephew. How old is his nephew today?
HumanEval [Chen et al., 2021]	Reasoning / Open-Ended	Python programming problems requiring function implementation based on a natural language description. <i>Example:</i> Write a function that returns the sum of two numbers.
MMLU [Li et al., 2023a]	Knowledge / Multiple-Choice	A massive multitask test consisting of multiple-choice questions from various branches of knowledge. <i>Example:</i> Who set the world record for the mile race in 1886? A. R Bannister, B. S Coe, C. J DiMaggio, D. WG George
CEVAL [Huang et al., 2023]	Knowledge / Multiple-Choice	A comprehensive Chinese evaluation suite for foundation models. <i>Example:</i> 下列各项中，应征收资源税的是_____。A. 人造石油 B. 某商贸企业零售的煤炭 C. 开采铁矿石同时开采的锰矿 D. 某联合企业进口的石油
CMMLU [Li et al., 2023a]	Knowledge / Multiple-Choice	A comprehensive Chinese multi-subject exam benchmark with 57 subjects. <i>Example:</i> 关系数据库中数据的逻辑结构是 (A) 树结构 (B) 维度表 (C) 层次结构 (D) 形状结构
BoolQ [Clark et al., 2019]	CommonSense / Multiple-Choice (Yes/No)	Reading comprehension questions with yes/no answers based on a passage. <i>Example:</i> Property tax – Property tax or ‘house tax’ is a local tax ... Is house tax and property tax are same?
CommonSenseQA [Talmor et al., 2019]	CommonSense / Multiple-Choice	A new multiple-choice question answering dataset that requires different types of commonsense knowledge to predict the correct answers . <i>Example:</i> Sammy wanted to go to where the people were. Where might he go? A. race track, B. populated areas, C. the desert, D. apartment, E. roadblock."

the active rate drops sharply from near 100% to a stable plateau. The remaining training focuses on optimizing the language modeling objective under the learned sparsity pattern.

B.3 More Baseline Comparison

We additionally compare BEAM with DynMoE [Guo et al., 2024], which replaces hard Top-K routing with sigmoid-gated expert selection based on token-expert affinity. Table 8 summarizes the results on all three evaluated models.

Table 8: Performance comparisons of DynMoE and BEAM relative to the original models.

Methods \ Tasks	Avg. K	Reasoning			Knowledge			CommonSense		Avg. (Acc. ↑)
		MATH	GSM8K	H_Eval	MMLU	CEVAL	CMMLU	BoolQ	CSQA	
<i>Qwen1.5-MoE-A2.7B</i>										
Qwen1.5-MoE $K=4$	4.00	23.04	57.47	50.61	59.28	74.15	75.18	72.63	81.33	61.71
DynMoE	30.06	10.72	45.03	31.10	42.94	37.60	39.35	60.89	61.51	41.14
BEAM ($\beta=0.01$)	1.56	24.78	55.50	53.05	58.75	70.47	69.18	78.32	80.84	61.36
<i>Qwen3-30B-A3B</i>										
Qwen3-30B-A3B $K=8$	8.00	58.28	88.02	82.93	81.80	83.56	83.69	86.76	86.24	81.41
DynMoE	61.66	19.46	66.49	39.02	40.64	36.42	36.51	58.50	51.11	43.52
BEAM ($\beta=0.01$)	4.23	55.16	85.52	81.71	80.09	81.46	81.53	88.07	86.40	79.99
<i>DeepSeekV2-Lite</i>										
DeepSeekV2-Lite $K=6$	6.00	20.02	62.70	43.90	55.04	55.26	60.93	75.20	68.14	55.15
DynMoE	30.50	0.04	1.36	0.00	5.11	6.63	0.41	8.81	6.39	3.59
BEAM ($\beta=0.01$)	2.61	20.36	60.27	46.95	56.65	54.12	60.42	76.57	65.11	55.06

DynMoE exhibits substantial instability in the post-training setting, as its learned gating tends to over-activate experts far beyond the original Top-K budget. Specifically, the average number of activated experts rises to 61.66 on Qwen3-30B-A3B (vs. Top-K = 8), 30.06 on Qwen1.5-MoE-A2.7B (vs. Top-K = 4), and 30.50 on DeepSeekV2-Lite (vs. Top-K = 6). This instability also leads to severe accuracy degradation, most notably on DeepSeekV2-Lite, where performance collapses from 55.15 to 3.59 average accuracy. This is likely because DynMoE completely replaces the original router architecture, making it ill-suited for post-training scenarios where preserving the pretrained routing structure is critical. In contrast, BEAM achieves substantially higher sparsity while retaining over 98% of the original model’s performance across all three models.

B.4 Layer-wise Masking Rank Analysis

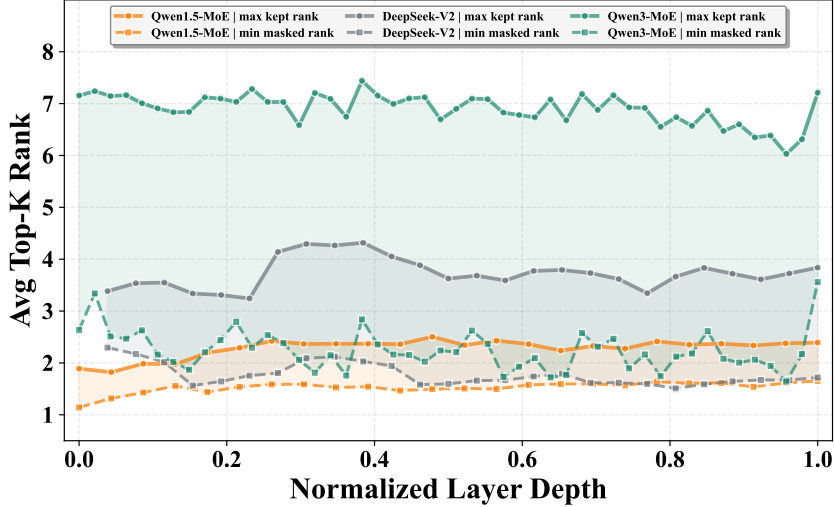


Figure 8: Layer-wise masking rank analysis across three MoE models. The shaded region between the min masked rank and max kept rank indicates the overlap zone where BEAM’s masking decisions are token-dependent.

To further investigate whether BEAM’s masking decisions follow routing rank, we record the minimum masked rank and maximum kept rank per layer across all three models (Figure 8). Across all layers and models, the min masked rank stays as low as 1–3, meaning that even highly-ranked experts are frequently pruned when redundant for a given token. Meanwhile, the max kept rank extends to the lower end of the Top-K range, confirming that low-ranked experts can be retained when critical. The wide overlap between masked and kept ranks demonstrates that BEAM’s decisions are driven by token-expert relevance rather than routing position.

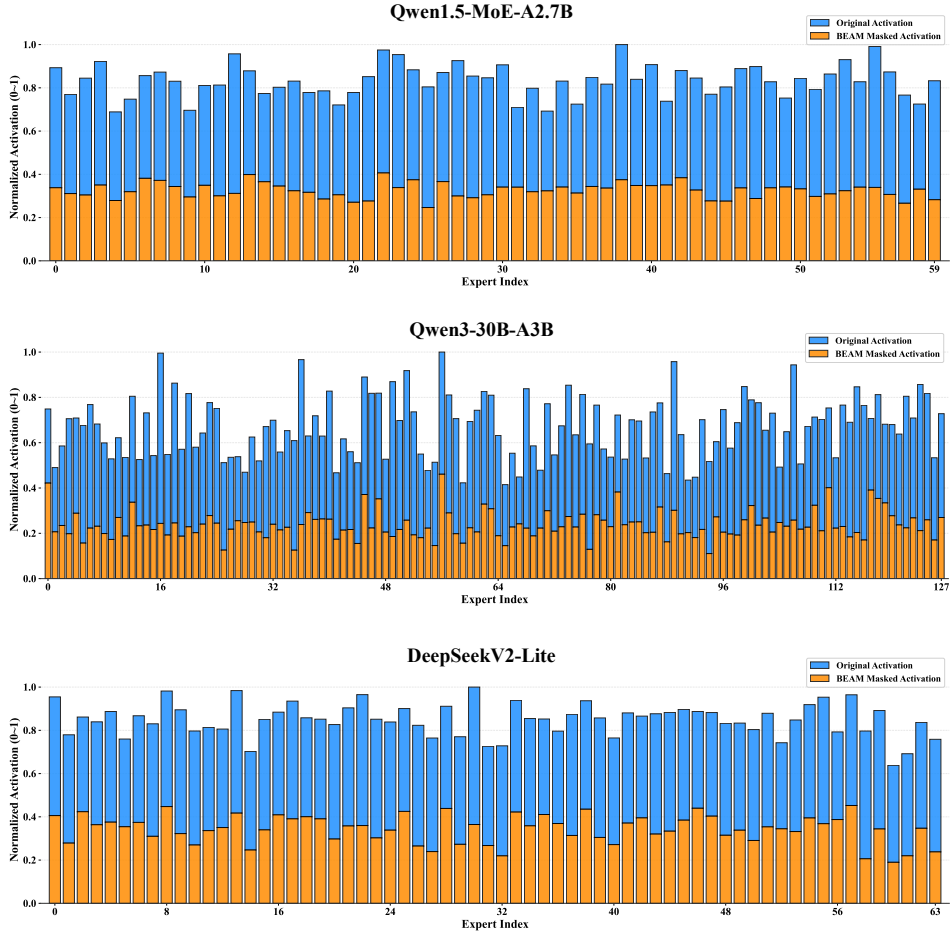


Figure 9: Expert load balance visualization of MoE models before and after BEAM fine-tuning.

B.5 Expert Load-Balance Analysis

To investigate BEAM’s impact on load balancing in MoE models, we visualize the utilization rates of experts for both original model and BEAM-augmented model during inference in our studied MoE models, as shown in Figure 9. The results demonstrate that the BEAM method performs uniform masking across experts, maintaining relatively balanced expert loads even on models such as Qwen3-30B-A3B that contains 128 experts. This finding highlights the applicability of the BEAM method to large-scale expert-parallel MoE models.

B.6 Task-specific Inference Speed Analysis

Table 9: Task-specific acceleration comparisons on Qwen3-30B-A3B.

Model	MATH	GSM8K	H_Eval	MMLU	CEVAL	CMMLU	BoolQ	CSQA	All
Qwen3-30B-A3B	2667s	329s	43s	980s	77s	460s	89s	46s	4691s
BEAM	2058s	247s	28s	709s	54s	330s	81s	36s	3543s
Speedup	1.30x	1.33x	1.53x	1.38x	1.42x	1.39x	1.10x	1.27x	1.32x

To further evaluate BEAM’s acceleration across tasks, we measure the inference speed of the BEAM-augmented Qwen3-MoE model ($\beta = 0.1$) and its baseline on several evaluation benchmarks using vLLM on a single NVIDIA H20 GPU. The results are summarized in Table 9. BEAM achieves consistent speedups across all tasks, indicating efficiency improvements in both prefill and decoding.

B.7 Token-Layer Sparsity Visualization

We visualize the per-token and per-layer expert activation patterns of Qwen1.5-MoE-A2.7B, DeepSeekV2-Lite, and Qwen3-30B-A3B on the same input prompt: “In only one sentence, what do you think of the future of AI?”. The results are shown in Figures 10, 11, and 12, which show significant differences in activation patterns across models and layers. Chat template tokens such as “You are a helpful assistant” activate almost no experts across all models. Notably, the degree of prefill-decode divergence varies by model: Qwen3 exhibits substantially more expert activation during decoding than prefill, Qwen1.5-MoE shows a moderate increase, while DeepSeekV2-Lite maintains largely consistent activation across both phases. For Qwen models, we also observe that prefill tokens mainly activate experts in shallow layers whereas decode tokens make stronger use of deeper layers, developing an encoder-decoder-like pattern where shallow layers handle knowledge encoding and deeper layers focus on reasoning.

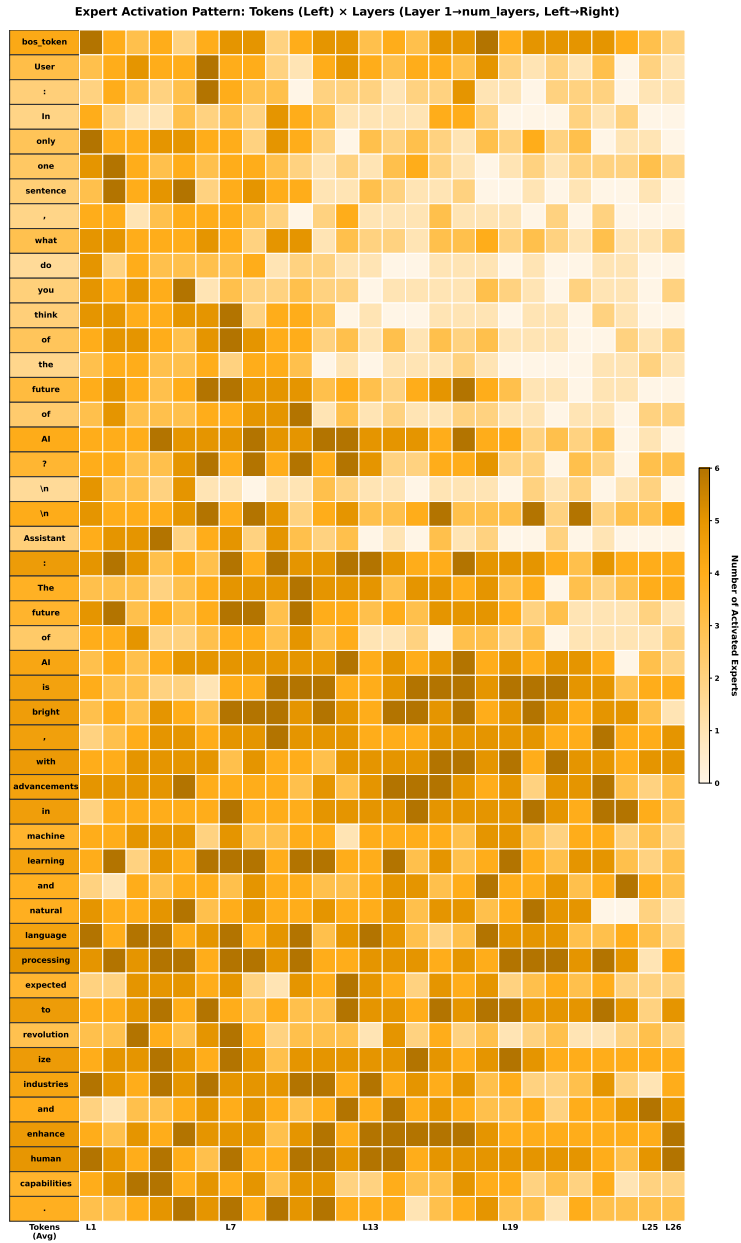


Figure 10: Per-token and per-layer expert activation heatmap for DeepSeekV2-Lite. Each cell indicates the number of activated experts for a token (vertical axis) at a given layer (horizontal axis).

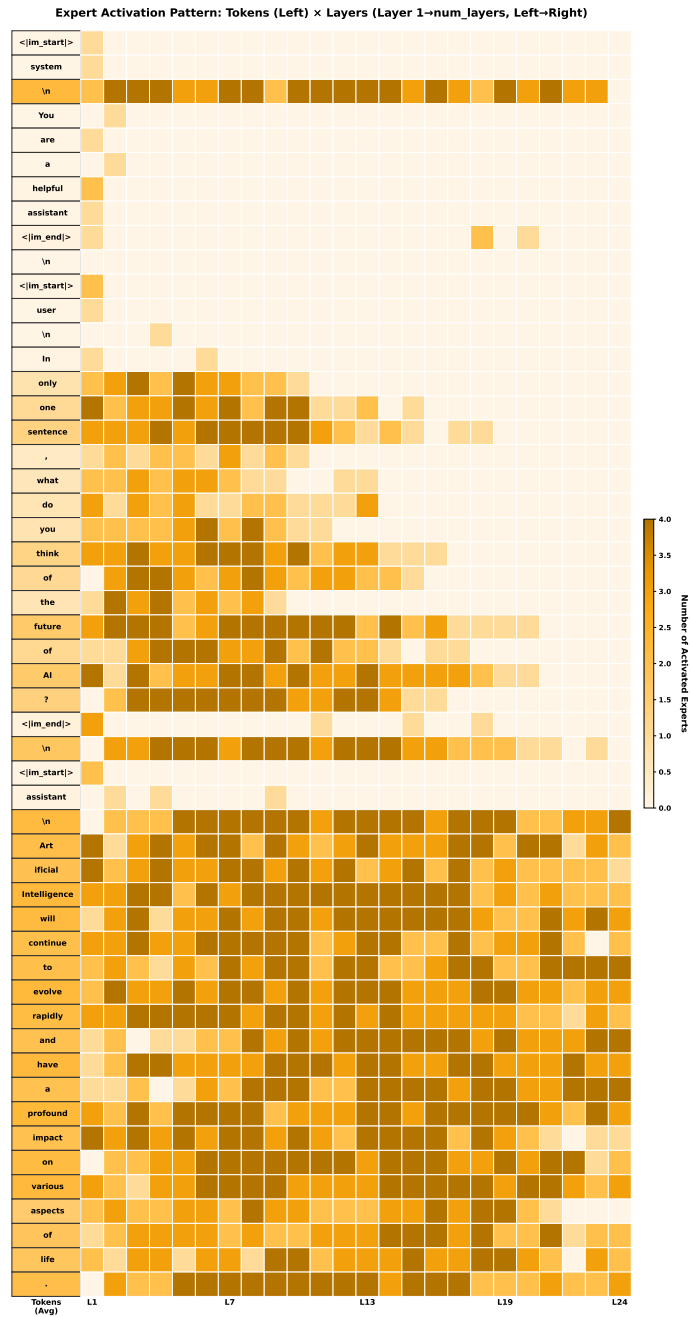


Figure 11: Per-token and per-layer expert activation heatmap for Qwen1.5-MoE-A2.7B. Each cell indicates the number of activated experts for a token (vertical axis) at a given layer (horizontal axis).

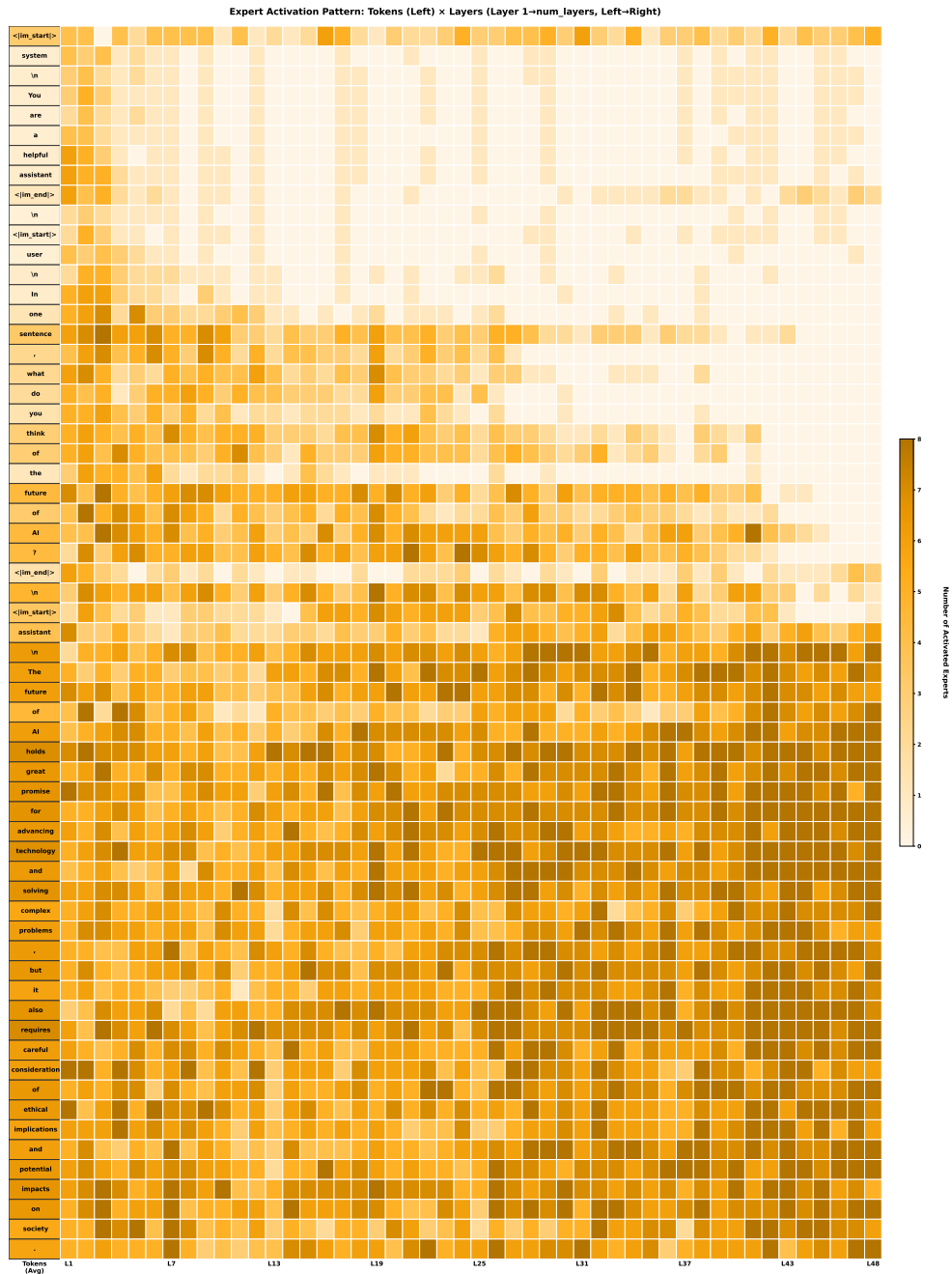


Figure 12: Per-token and per-layer expert activation heatmap for Qwen3-30B-A3B. Each cell indicates the number of activated experts for a token (vertical axis) at a given layer (horizontal axis).